IOPscience iopscience.iop.org

Home Search Collections Journals About Contact us My IOPscience

Isochronal annealing behaviour of defects induced by swift oxygen ions in high-resistivity p-type silicon

This article has been downloaded from IOPscience. Please scroll down to see the full text article.

2007 J. Phys.: Condens. Matter 19 216206

(http://iopscience.iop.org/0953-8984/19/21/216206)

View the table of contents for this issue, or go to the journal homepage for more

Download details:
IP Address: 129.252.86.83
The article was downloaded on 28/05/2010 at 19:05

Please note that terms and conditions apply.

IOP PUBLISHING JOURNAL OF PHYSICS: CONDENSED MATTER

J. Phys.: Condens. Matter **19** (2007) 216206 (9pp) doi:10.1088/0953-8984/19/21/216206

Isochronal annealing behaviour of defects induced by swift oxygen ions in high-resistivity p-type silicon

S K Chaudhuri[1], **K Goswami**[2], **S S Ghugre**[1] **and D Das**[1]

[1] UGC-DAE Consortium for Scientific Research, Kolkata Centre, III/LB-8, Bidhannagar, Kolkata-700098, India

[2] Department of Physics, Jadavpur University, 188 Raja S C Mallik Road, Kolkata-700032, India

E-mail: ddas@alpha.iuc.res.in

Received 24 November 2006, in final form 4 April 2007
Published 27 April 2007
Online at stacks.iop.org/JPhysCM/19/216206

Abstract

High-resistivity detector-grade p-type silicon wafers have been implanted with swift oxygen (O^{6+}) ions under two different conditions. One of the wafers was implanted effectively with a pulsed beam of varied energy (3–140 MeV) to a total fluence of 5×10^{15} ions cm^{-2}, resulting in a depth-wise near-uniform implantation profile. The other wafer was directly irradiated with a 140 MeV steady oxygen beam to the same fluence. Radiation-induced defects produced in the samples and their isochronal annealing behaviours were studied by positron annihilation lifetime spectroscopy and Doppler broadening of positron annihilation radiation measurements. The lifetime spectra of the irradiated samples were fitted with three lifetimes. Trapping model analysis was carried out with the de-convoluted lifetimes to characterize the defect states. The defect-related lifetime τ_2 in both the irradiated samples was found to be due to an admixture of divacancy (V_2) and divacancy–oxygen (V_2O) complexes. A marked difference in the defect reordering process has been observed between the two samples, which is explained by taking into account the effect of injection annealing by minority carriers which are produced by the energetic beam prior to forming displacement damage.

1. Introduction

Radiation effects in materials of technological importance is a widely studied area, initiated in the early 1940s by Wigner and collaborators [1]. Displacement damage in silicon was first studied, according to the records, by Johnson and Lark-Horovitz in 1949 [2]. Since then, defect studies in silicon have remained a prime interest in the field of semiconductors. Silicon, among all semiconductors, has proven itself as the most promising material that can be used as a radiation detector, and it is expected to remain so for a long time in the future.

The effect of high-energy particle bombardment in silicon is a complex phenomenon to study, since the mechanism of defect creation and the ultimate damage produced depend

© 2007 IOP Publishing Ltd Printed in the UK

on parameters like ion type, energy, beam current, fluence, irradiation temperature, doping concentration of the target, etc. The prime interest of radiation-detector scientists and engineers is to correlate the nature of defects with device performance in terms of resolution, operating voltage, leakage current, etc, and to ensure radiation hardness of the device by adopting suitable means. Oxygen enrichment of silicon wafers prior to detector fabrication is a well-established technique to increase the radiation hardness of silicon detectors [3]. The conventional process of oxygen enrichment is a thermal diffusion process, which is time consuming and involves the risk of contamination by unwanted elements. An alternative fast and clean process can be adopted via direct oxygen implantation in the crystal [4]. Implantation by high-energy (>100 MeV) oxygen ions ensures that the projectile is embedded deep inside (>100 μm) the lattice, which is needed for fabrication of a practical detector with the irradiated wafer [3]. However, ion implantation causes lattice defects in the crystal that need to be annealed out prior to device fabrication. The defect recovery of the crystal depends on the nature of the primary damage created by the energetic particles and its interaction with the oxygen/impurity atoms. Hence, the study of radiation damage in silicon caused by high-energy ions and its recovery under thermal annealing is of prime importance. Implantation with ions of single energy results in a non-uniform concentration of oxygen along the path of the projectile because almost all the oxygen atoms are located at the end of the path range with a short spread caused due to a straggling effect. A more or less uniform concentration of oxygen along the projectile path can be realized by implanting the sample with variable-energy ions because the particles with different energies are stopped at different depths in the sample.

The present paper focuses on identification of defects produced by high-energy oxygen implantation on detector-grade p-type silicon irradiated under two different conditions, and compares the corresponding defect recovery characteristics under thermal annealing. One of the wafers was irradiated with an oxygen (O^{6+}) beam whose energy was degraded stepwise from 140 to 3 MeV; this is denoted as sample S1. A rotating degrader (details are given in section 2) was used for this purpose and the resulting beam was effectively of pulsed nature. The other wafer was irradiated directly with 140 MeV oxygen ions, and is denoted as sample S2. All irradiations were done at room temperature under high vacuum. Other parameters like beam current, irradiation temperature, etc, were kept the same while irradiating both the wafers.

Positron annihilation lifetime spectroscopy (PALS) and single-detector Doppler broadening of the annihilation radiation (DBAR) have been carried out to identify the defects and to study their dynamics under isochronal annealing. Positron annihilation spectroscopy is a powerful tool for identifying microstructural defects in a solid [5]. An interesting difference in the annealing behaviour between S1 and S2 was observed which has been attributed to their different ion-implantation conditions. The investigation is of technological importance and is expected to provide important information in the field of defect studies in semiconductors with swift heavy ions (SHIs), which still requires a lot of experimentation for substantial comprehension.

2. Experimental methods

P-type detector-grade silicon wafers (resistivity ∼2000 Ω cm) of thickness around 500 μm and diameter about 15 mm were sliced from an ingot along the ⟨111⟩ crystal planes and irradiated with 140 MeV oxygen ions (O^{6+}) up to a fluence of 5×10^{15} ions cm^{-2} using the beam-line of the Variable Energy Cyclotron Centre (VECC), Kolkata, India. The following technique was adopted for varying the energy. An aluminium wheel with 14 trapezoidal slots along its periphery was placed in front of the target. The wheel was fitted with a low-speed electric motor moving with a constant speed throughout the irradiation. This ensures that the beam

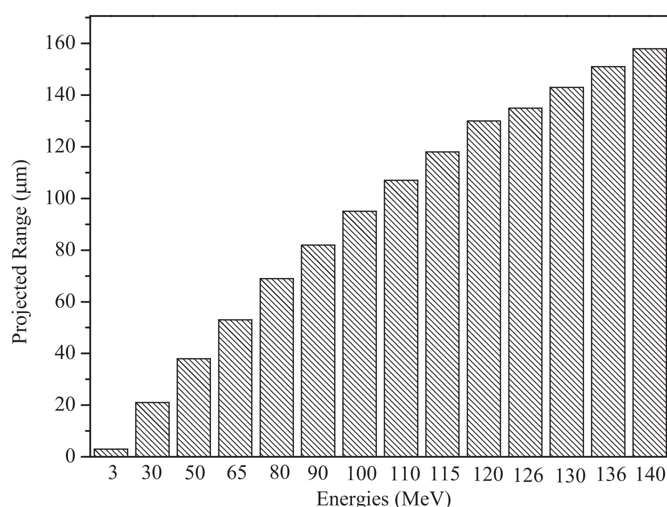

Figure 1. Beam energies and their corresponding ranges obtained after using rotating degrader.

passes through the slots one at a time and that each slot faces the beam in a cyclic manner. All the slots, except one, were covered with aluminium foils of varied thickness to obtain a layer-wise distribution of the projected range of oxygen ions starting from 3 to 158 μm. The resulting beam acted therefore as a pulsed beam, the pulse width being 0.4 s with a repetition period (the time gap between two pulses of same energy) of 7 s. Figure 1 gives a histogram of the beam energies and their corresponding projected ranges, calculated using SRIM 2003 [6].

For PALS and DBAR measurements, about 12 μCi ^{22}Na activity was deposited and dried on a thin aluminium foil and was covered with an identical foil. This assembly was used as the positron source. The PALS system used was a standard fast–fast coincidence set-up with two identical 1 inch tapered off BaF_2 scintillator detectors fitted with XP2020Q photomultiplier tubes. The time resolution obtained using a ^{60}Co source with ^{22}Na gates was 298 ps. A total of more than 1 million counts were recorded for each lifetime spectrum, the typical acquisition time being 5 h. All lifetime spectra were analysed using the PATFIT 88 [7] program after background and source corrections. The source correction was carried out following the procedure adopted by Staab *et al* [8]. It is to be mentioned here that a fraction of positrons passes through the irradiated layer without annihilating therein. These positrons annihilate with bulk electrons in the defect-free region. The contribution from these annihilations has not been included in the source correction. Up to an annealing temperature of 600 °C, all lifetime spectra of the irradiated samples were deconvoluted using one Gaussian resolution function with three exponential lifetimes. Beyond 600 °C, a single-component fit gave satisfactory results.

The DBAR spectra were recorded for 2 h using a single HPGe detector with an energy resolution of 1.9 keV for 662 keV gamma rays from a ^{137}Cs standard source. The Doppler broadened energy spectra were analysed using the code SP (version 1.0) [9] to calculate the S-parameter. This code uses a Gaussian fitting of the experimental points and a background correction prior to the final calculation. The S-parameter is defined as the ratio of the area under a fixed central window around the peak to that under the annihilation line. A central window span of 0.8 keV on either side of the centroid of 511 keV peak has been used in the present work. Each annealing was carried out in vacuum ($\sim 10^{-5}$ mbar) for 30 min from 100 to 675 °C.

Several data were retaken and reanalysed, and the resolution and peak position were monitored intermittently to check the reproducibility of the results and the stability of the spectrometer. Reasonably good reproducibility and stability of the spectrometer were observed during the three-week long experiment. The variance of the fit was minimized to obtain the best fit and at the same time the standard deviations of the individual lifetime parameters were checked not to give abnormally large values even if showing a lesser variance of the overall fit.

3. Results and discussions

3.1. Pre-irradiation scenario

The PALS spectrum of the unirradiated wafer was fitted with a single component to get a lifetime of 219 ps, which is close to the bulk lifetime of positrons in silicon as reported by others [10]. The S-parameter was calculated to be 0.5203.

3.2. Defect creation during irradiation and reordering processes

During irradiation, several kinds of defect formation and interactions are possible depending on particle type and energy. Soon after their creation, these defects can simply recombine to disappear (forward annealing) or they can migrate and reorder to more stable configurations (reverse annealing). The different channels through which defect annealing or reordering normally takes place can be described as follows:

(i) $V - I$ (recombination).
(ii) $V + V \rightarrow V_2$ (divacancy formation).
(iii) $I + I \rightarrow I_2$ (di-interstitial formation).
(iv) $I_2 + V \rightarrow I$ (complex recombination).
(v) $V + O \rightarrow VO$ (A centre formation).
(vi) $V_2 + O \rightarrow V_2O$ (higher order complexes),

where V and I stands for vacancy and interstitial respectively, O is oxygen atom.

These processes are completed in a time of the order of several minutes to 1 h after the irradiation, leaving behind stable defects often referred to as permanent defect [11–13]. These short-term annealing processes are strongly influenced by the presence of free charge carriers, a phenomenon known as injection annealing [14]. These charge carriers may be introduced by electrical injection or excitation due to ionizing radiation. Prior to producing displacement damage, the energetic beam will excite electron–hole pairs, which can enhance the defect reordering process. In both samples S1 and S2, defect creation and simultaneous reordering processes take place throughout the irradiation. In sample S1, the recombination processes are expected to be more pronounced due to larger magnitude of injection annealing than that in sample S2, and these are discussed in detail later in the text.

3.3. Post-irradiation scenario

The lifetime spectra of the as-irradiated samples were fitted with three lifetime components. The shortest lifetime τ_1 was assigned to the reduced Bloch state residential lifetime of positrons annihilating with the bulk electrons, with I_1 being the corresponding intensity. The intermediate lifetime τ_2 with intensity I_2 was attributed to positrons annihilating at the defect sites, and the longest lifetime τ_3 with intensity I_3 was attributed to positrons annihilating via pick-off annihilations of ortho-positronium. The ortho-positronium formation may take place at the sample surface or in voids within the sample created due to irradiation. Because of the low

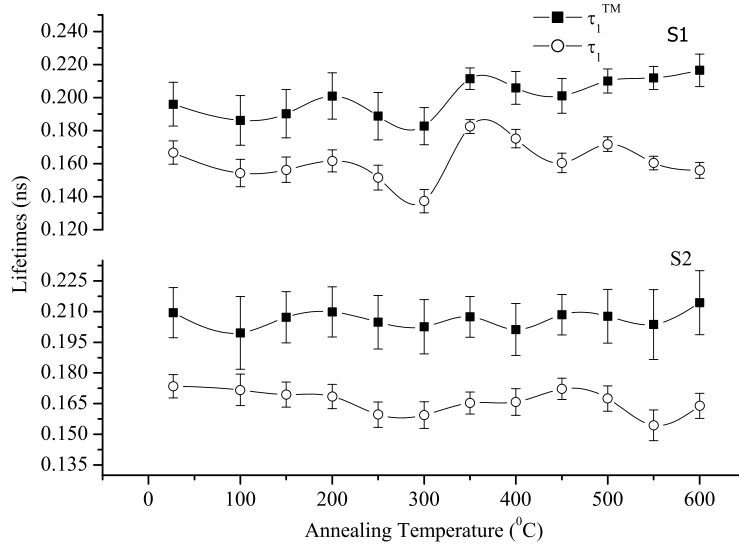

Figure 2. Comparison of experimental value of τ_1 and calculated value of τ_1 from two-state trapping model (τ_1^{TM}).

Table 1. Positron annihilation parameters for the unirradiated and the irradiated samples.

Sample	τ_1 (ps)/I_1 (%)	τ_2 (ps)/I_2 (%)	τ_3 (ns)/I_3 (%)	S
Unirradiated	219 ± 1	—	—	0.5203 ± 0.0007
S1	$166 \pm 7/60 \pm 6$	$294 \pm 11/38 \pm 6$	$2.33 \pm 0.06/2 \pm 0.05$	0.5348 ± 0.0008
S2	$174 \pm 5/72 \pm 6$	$300 \pm 16/26 \pm 6$	$2.36 \pm 0.06/2 \pm 0.05$	0.5290 ± 0.0008

intensity of this component (<2%), its variation during the isochronal annealing studies has not been discussed. Table 1 shows the values of lifetime parameters for the samples S1 and S2 along with S-parameters evaluated from the DBAR measurements.

3.3.1. Trapping model analysis. To get more insight into the positron trapping sites in the irradiated samples, a two-state trapping model [15, 16] analysis was carried out with the deconvoluted lifetimes. The two states correspond to a bulk state and a defect-related state. As per this model, the experimental lifetimes τ_i and the intensities I_i (i = 1, 2) are related to the characteristic lifetime τ_b and τ_d by

$$\tau_1^{-1} = \tau_b^{-1} + K \tag{1}$$

$$I_2 = 1 - I_1 = \frac{K}{K + \lambda_b - \lambda_d} \tag{2}$$

where τ_b is the bulk lifetime, $\tau_d = \tau_2$ is the characteristic of the defect trapping a positron, K is the trapping rate and λ_b and λ_d are the annihilation rates in the bulk and in the defects respectively. The trapping rate was calculated at different annealing temperatures using equation (2) with the experimentally obtained values of τ_2 and I_2, and the theoretical bulk lifetime (τ_1^{TM}) was calculated from the relation $\tau_1^{TM} = (\lambda_b + K)^{-1}$. The value of λ_b was taken as $1/219$ ps^{-1}. Figure 2 shows a comparison between τ_1^{TM} and the experimental lifetime τ_1 for both S1 and S2. It is evident from the figure that for both samples the values of τ_1^{TM} at

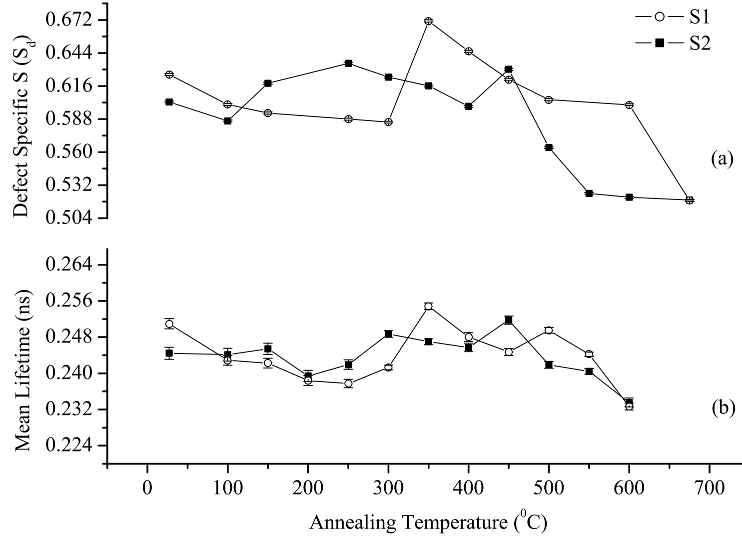

Figure 3. Variation of (a) defect-related S-parameter, (b) mean lifetime with annealing temperature. (In graph (a) experimentally determined S-parameter values at 675 °C are included for comparison.)

all the temperatures are much higher than the corresponding experimentally observed τ_1 value, indicating that a two-state trapping model is not adequate in the present case, and pointing to the presence of more than one defect state in the irradiated sample. However, the inclusion of an additional lifetime in the deconvolution procedure was not possible, probably because the defect-related lifetimes are rather close, and hence a three-state trapping model has not been tried.

After irradiation, the defect-related lifetime component (τ_2) in S1 was found to be 294 ps. This value is higher than the lifetime reported for V_2O (286 ps) but substantially lower than the lifetime of V_2 (305 ps) [17, 18]. It is therefore proposed that the observed lifetime corresponds to a mixed state comprising both divacancy (V_2) and divacancy–oxygen (V_2O) complexes. For sample S2, τ_2 was found to be 300 ps, which has been assigned to the same type of defect as in S1. The slightly higher value of τ_2 in the case of S2 in comparison with that of S1 is believed to arise due to the presence of a higher fraction of V_2-type defects compared to V_2O defects in the sample. A similar kind of assignment had been reported by Bondarenko *et al* [19] for neutron-irradiated high-resistivity float-zone-grown p-type silicon.

3.3.2. Isochronal annealing studies. Figure 3(a) shows the variation of defect-specific S-parameter (S_d) with annealing temperature. The defect-specific S-parameter has been calculated using the following equation.

$$S = (1 - f)S_{bulk} + fS_d \quad (3)$$

where S is the experimentally obtained values of S-parameter and f represents the fraction of trapped positrons and is given by

$$f = \frac{K}{\lambda_{bulk} + K} \quad (4)$$

where K is the trapping rate obtained from equation (2) and S_{bulk} is the value of S-parameter for the defect-free sample. S_d for S1 shows an increase at 350 °C followed by a gradual

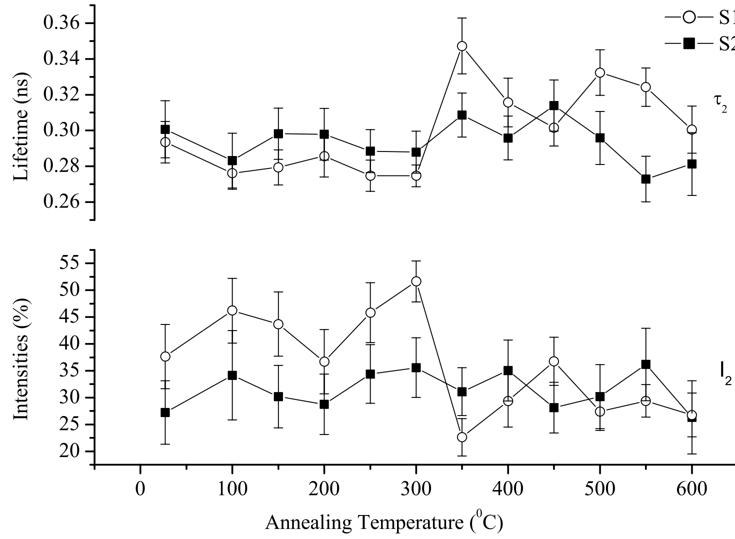

Figure 4. Variation of τ_2 and I_2 with annealing temperature.

decrease with increase of annealing temperature, indicating gradual annealing out of vacancy-type defects. For sample S2, a rise of lesser magnitude has been seen at 450 °C and a gradual fall at higher temperature. After annealing at 675 °C, the value of S-parameter for both the samples almost matched the value obtained for the unirradiated sample. This points to the fact that almost all the defects are annealed out at this temperature. The lifetime analysis (to be discussed later) also supports these trends.

Figure 3(b) shows the variation of mean lifetime τ_m of both samples with annealing temperature. The mean lifetime was calculated using the formula

$$\tau_m = \frac{\sum_{i=1}^{3} \tau_i I_i}{\sum_{i=1}^{3} I_i}. \quad (5)$$

Since τ_m also gives the average defect contribution, its variation with annealing temperature is expected to be more or less same as with the S-parameter. For sample S1, τ_m shows a pronounced increase at 350 °C, indicating some sort of reverse annealing leading to an agglomeration of defects. Further annealing up to 600 °C reduces the mean lifetime gradually, pointing to annealing out of defects. For sample S2, τ_m showed a marginal increase around 450 °C, indicating less pronounced reverse annealing. Beyond that, τ_m decreases steadily, pointing to gradual annealing out of defects as observed for sample S1.

The above discussion on the S-parameter and the mean lifetime (τ_m) gives the overall variation of microstructural defects with annealing temperature. For a better understanding of the defect dynamics, the defect-related lifetime, τ_2, and the corresponding intensity I_2 must be observed carefully. Figure 4 shows the variation of τ_2 and I_2 with annealing temperature for both samples. Let us first consider the case of sample S1. Up to 350 °C, the lifetime values for sample S1 remain more or less the same, signifying that the corresponding defect state comprising divacancy and divacancy–oxygen complexes ($V_2 + V_2O$) is stable up to that temperature. A sharp increase in τ_2 has been noticed at 350 °C. The corresponding intensity I_2 has also dropped considerably from 45% to 20% at that temperature. These observations point to agglomeration of defects to form larger clusters. The lifetime $\tau_2 = 347$ ps found after annealing at 350 °C is closer to that of six-vacancy cluster (V_6) [20, 21]. A first-principles

calculation based on the density functional theory showed that the formation of V_6 in silicon is energy-wise favourable [21].

At 350 °C, the divacancies (V_2) are expected to anneal out [19], whereas V_2O is thermally stable [22]. Therefore, the sharp increase in τ_2 can be assigned to the annealing of divacancies through their agglomeration to form more stable defects like V_6.

This six-vacancy cluster is found to be dissociating slowly in the temperature range 350–450 °C as τ_2 decreases and I_2 increases in that temperature interval. It may be mentioned here that the dissociation of V_6 may take place through the formation of (i) V_5+V_1, (ii) V_4+V_2 and (iii) V_3+V_3. Out of these, the first one is more probable as the corresponding dissociation energy is minimum [23]. The released monovacancies or divacancies will immediately anneal out at the said temperature, but higher-order vacancies may form oxygen–vacancy complexes like $V_mO_n (m > 3, n < m)$ [24], which are stable at that temperature. Above 450 °C, the annealing behaviour therefore is governed by the simultaneous presence of V_2O-type defects created during irradiation and V_mO_n formed subsequently during isochronal annealing.

Now let us consider the variation of τ_2 with temperature for sample S2. As discussed earlier, this sample, before being subjected to isochronal annealing, also contains V_2 and V_2O types of defect. But unlike in S1, the aggregation of V_2 to form higher-order vacancy clusters at 350 °C was not seen, as τ_2 did not show any appreciable increase at that temperature. This contrasting behaviour in the two samples can be explained as follows. Calculations using SRIM 2003 code showed that for oxygen ions of energy greater than 1 MeV, the electronic stopping power in silicon decreases with increase of ion energy. Because of the special experimental condition (use of a rotating degrader), the average energy of the beam is lower in the case of sample S1 compared with the same for sample S2. Therefore, a larger number of minority carriers (electrons) are expected to be produced in the case of sample S1 by the process of ionization. This in turn leads to enhanced injection annealing, as discussed earlier in section 3.2. Moreover, in the case of S1, because of the varied energy of the beam a defect region created by a beam of particular energy is subject to injection annealing by minority carriers produced by beams of successive higher energy. As a result of these, a substantial reduction in the number of interstitials takes place in the sample via rapid recombination, prohibiting thereby the formation of large interstitial clusters. In the case of sample S2, because of the higher average energy of the beam the minority carrier injection level is lower than that in S1, and the formation of large interstitial clusters (immobile at room temperature) is expected to dominate over the recombination process during irradiation. These large interstitial clusters become mobile at higher temperature (∼350 °C) and take part in divacancy annealing by recombination process, hence prohibiting divacancy agglomeration and formation of clusters like V_6.

Another point to be noted is that the intensity (I_2) of the defect-related state for sample S1 is distinctly higher than that for sample S2, particularly below 300 °C (figure 4). This indicates a higher concentration of the corresponding defects in S1, which most probably is due to the implantation by variable energy beam. In the case of S2, the implantation is by a 140 MeV beam, and the defects are mainly created deep inside the specimen near the end of the projectile range. In S1, the defects are uniformly distributed in the specimen and hence the probability of seeing them by positrons is more, which results in the higher value of I_2.

4. Conclusion

Defects formed in p-type silicon irradiated with high-energy oxygen ions under two different implantation conditions and their dynamics under isochronal annealing have been studied by positron annihilation spectroscopy. The reduced bulk lifetime τ_1 calculated from a two-state

trapping model did not give a satisfactory fit to the experimentally determined τ_1 values. This led to the conclusion that the defect-related lifetime (τ_2) corresponds to an admixture of more than one defect state. This mixed state was proposed to be composed of V_2 and V_2O. A marked difference in the annealing behaviour of τ_2 between the sample irradiated with a beam of varied energy (3–140 MeV) and that irradiated directly with a 140 MeV beam has been observed around 350 °C. This difference has been explained by taking into account the effect of injection annealing by minority carriers, which is more pronounced in the case of the sample irradiated with varied energy. Final annealing out of the irradiation-induced defects in both samples was observed at 675 °C.

Acknowledgments

The authors would like to thank Dr P M G Nambissan and Professor S Bhattacharya of SINP, Kolkata, for lending the rotating degrader facility and also all staff of VECC, Kolkata for providing the 140 MeV oxygen beam. Thanks are also due to Mr B K Nath, Mr Samrat Mukherjee and Mr P V Rajesh for various help at different stages of the experiment.

References

[1] Wigner E P 1946 *J. Appl. Phys.* **17** 857
[2] Johnson W E and Lark-Horovitz K 1949 *Phys. Rev.* **76** 442
[3] Lindström G *et al* 2001 *Nucl. Instrum. Methods* A **465** 60
[4] Chaudhuri S K, Mukherjee S, Rajesh P V, Ghugre S S and Das D 2005 *Physica* B **362** 249
[5] Krause-Rehberg R and Leipner H S 1999 *Positron Annihilation in Semiconductors* (Berlin: Springer) chapter 3 p 127
[6] Ziegler J F, Biersack J P and Littmark U 1985 *The Stopping and Range of Ions in Solids* (Oxford: Pergamon)
[7] Kirkegaard P and Eldrup M 1972 *Comput. Phys. Commun.* **3** 240
[8] Staab T E M, Somieski B and Krause-Rehberg R 1996 *Nucl. Instrum. Methods* A **381** 141
[9] http://positronannihilation.net/software.html
[10] Dannefaer S 1982 *J. Phys. C: Solid State Phys.* **15** 599
[11] Sander H H and Gregory B L 1966 *IEEE Trans. Nucl. Sci.* **14** 116
[12] Sander H H and Gregory B L 1971 *IEEE Trans. Nucl. Sci.* **18** 250
[13] Lazanu S and Lazanu I 2004 *Phys. Scr.* **69** 376
[14] Gregory B L 1965 *J. Appl. Phys.* **36** 3765
[15] Seeger A 1973 *J. Phys. F: Met. Phys.* **3** 248
[16] Vehanen A, Hautojarvi P, Johansson J and Yli-Kauppila J 1982 *Phys. Rev.* B **25** 762
[17] Kuriplach J, Morales A L, Dauwe C, Segers D and Sob M 1998 *Phys. Rev.* B **15** 10475
[18] Makhov D V and Lewis L J 2005 *Phys. Rev.* B **71** 205215
[19] Bondarenko V, Krause-Rehberg R, Feick H and Davia C 2004 *J. Mater. Sci.* **39** 919
[20] Saito M and Oshiyama A 1995 *Phys. Rev.* B **53** 7810
[21] Staab T E M, Haugk M, Sieck A, Fraunheim Th and Leipner H S 1999 *Physica* B **273/274** 501
[22] Kawasuso A, Hasegawa M, Suezawa M, Yamaguchi S and Sumino K 1995 *Appl. Surf. Sci.* **85** 280
[23] Hastings J L, Estreicher S K and Fedders P A 1997 *Phys. Rev.* B **56** 10215
[24] Pi X D, Burrows C P, Coleman P G, Gwilliam R M and Sealy B J 2003 *J. Phys.: Condens. Matter* **15** S2825